Available online at www.sciencedirect.com

ScienceDirect

Energy Procedia 45 (2014) 12 – 21

Energy Procedia

68th Conference of the Italian Thermal Machines Engineering Association, ATI2013

Modeling and simulation of an isolated hybrid micro-grid with hydrogen production and storage

Giorgio Cau[a], Daniele Cocco[a], Mario Petrollese[a]*

[a]*Department of Mechanical, Chemical and Materials Engineering, University of Cagliari, via Marengo 2, 09123, Cagliari, Italy*

Abstract

This work relates the study of system performance in operational conditions for an isolated micro-grid powered by a photovoltaic system and a wind turbine. The electricity produced and not used by the user will be accumulated in two different storage systems: a battery bank and a hydrogen storage system composed of two PEM electrolyzers, four pressurized tanks and a PEM fuel cell. One of the main problems to be solved in the development of isolated micro-grids is the management of the various devices and energy flows to optimize their functioning, in particular in relation to the load profile and power produced by renewable energy systems depending on weather conditions. For this reason, through the development and implementation of a specific simulation program, three different energy management systems were studied to evaluate the best strategy for effectively satisfying user requirements and optimizing overall system efficiency.

Keywords: Hydrogen Storage; Stand-alone Power Systems; Renewable Energy Sources; Hydrogen from RES; Energy Management Strategy

1. Introduction

The use of renewable energy sources as an alternative to conventional fossil fuels is one of the goals set by the European Union with the approval of the so-called "EU climate and energy package" in 2008 [1]. In recent years, the use of related technologies has greatly increased in Italy. In 2012, energy production from renewable energy sources

* Corresponding author. Tel.: +39-070-675-5724; fax: +39-070-675-5717.
*E-mail address:*petrollese@unica.it

doi:10.1016/j.egypro.2014.01.003

Nomenclature

Photovoltaic system

I_{PV}	(A) photovoltaic panel current
V_{PV}	(V) photovoltaic panel voltage
I_{SC}	(A) photovoltaic cell short-circuit current
I_0	(A) saturation current
R_S	(Ω) series cell resistance
R_P	(Ω) parallel cell resistance
V_T	(V) thermal voltage
N_{CELL}	number of solar cell for a single panel

Wind turbine

v_{WT}	(m/s) wind speed at wind turbine hub height
v_{AN}	(m/s) wind speed recorded from anemometer
z_{WT}	(m) height of the turbine hub
z_{AN}	(m) height of the anemometer
P_{WT}	(W) power produced by wind turbine

Batteries

V_B	(V) battery voltage
E_B	(V) open-circuit voltage
$E_{B,0}$	(V) open-circuit voltage under standard conditions
K	(V) polarization voltage
Q_B	(Ah) battery capacity
$I_{B,t}$	(Ah) time integral of the battery current ($I_{B,t} = \int I_B dt$)
A, B	constants linked to the exponential term

Hydrogen storage system

n_{H2}	(mol/s) produced hydrogen flow
N_C	number of cells in parallel (called stack)
F	Faraday's constant
η_F	Faraday's efficiency
V_{EL}	(V) electrolyzer voltage
I_{EL}	(A) electrolyzer current
T_{EL}	(K) electrolyzer operating temperature
p_S	(Pa) hydrogen tank pressure
T_S	(K) stored hydrogen temperature
v_S	(m^3) overall tank volume
MM_{H2}	(kg/mol) molar mass of hydrogen
V_{FC}	(V) fuel cell voltage
I_{FC}	(A) fuel cell current
T_{FC}	(K) fuel cell operating temperature
E_{Nernst}	(V) Nernst potential
η_{EL}	electrolyzer efficiency
η_{FC}	fuel cell efficiency

Cost and lifetime

$C_{B,IN}$	(€) capital cost of battery
$C_{EL,IN}$	(€) capital cost of electrolyzer
$C_{FC,IN}$	(€) capital cost of fuel cell
$C_{O\&M,EL}$	(€/h) O&M cost of electrolyzer
$C_{O\&M,FC}$	(€/h) O&M cost of fuel cell
L_{EL}	(h) electrolyzer lifetime
L_{FC}	(h) fuel cell lifetime

(RES) represented 28.2% of electricity consumption and 13% of total consumption [2]. The main contribution comes from wind turbines (with an annual production of 13.9 TWh in 2012) and photovoltaic systems (18.8 TWh in 2012), characterized by rapid growth in recent years. One of the main problems of these systems is the uncertainty of the primary source (solar radiation and wind), which does not ensure a reliable supply especially at night and during the low insolation periods. In this context, the development of storage systems assumes fundamental importance. The use of hydrogen storage systems as an alternative or in addition to the use of electric batteries has been the subject of studies and research activities in recent years. In fact, water electrolysis processes produce hydrogen from electrical energy, and optionally oxygen, which can then be converted into electrical energy by a fuel cell. One of the advantages of hydrogen is its versatility of use in both stationary processes, such as storage and back-up systems, and in the transport sector. A further advantage is the absence of pollutants in the conversion process, except for NO_x.

This paper deals with some aspects of energy management in isolated systems exclusively powered by renewable sources. These solutions can be applied only in specific cases where the grid extension is not possible or very expensive, such as isolated telecommunications base stations, water pumping, irrigation etc. In the future, with the development of more efficient technologies and lower costs owing to economies of scale, these solutions will arouse real interest also for household applications. In the literature, several studies are available on the modeling and simulation of isolated hybrid systems with hydrogen storage [3-7]. Ulleberg [3] shows how the performance of these systems is highly dependent on the management and control of storage devices. Several studies in the literature [4,5] use the state of charge (SOC) of batteries as a decision variable. Therefore the operation of the hydrogen storage system will depend on the state of charge of the battery bank. In this case, the control system is very reliable, but on the other hand the storage system is not optimized from an economic point of view. Dufo-Lopez et al. [6] propose a different control strategy based on the minimization of energy cost. As highlighted by Castañeda et al. [7] this logic leads to a higher utilization of the hydrogen system compared to the previous strategies.

Table 1. Main components and characteristics of the micro-grid

Photovoltaic system		**Electrolyzer**		**Batteries**	
Panel peak power	0.225 kW	H_2 Net Production Rate:	1.05 Nm^3/h	Nominal voltage	12 V
Efficiency	18.1%	Delivery Pressure	13.8 barg	Rated Capacity (C100)	270 Ah
Solar cells	72 monocrystalline	Nominal power	6 kW	Batteries per string	4
Panel number	36	Number of cell	20	Max. Charge Current	48 A
Wind turbine		**Fuel Cell**		**Hydrogen Tank**	
Rated power @ 14 m/s	3 kW	Nominal power	5 kW	Number	4
Configuration	3 blades, vertical axis	H_2 rated consumption	65 Nl/min	Volume/Tank	1 m^3
Rotor diameter	3 m	Nominal voltage	48 V_{DC}	Maximum operating pressure	22 bar
Hub height	5.8 m	Nominal current	115 A		

This paper focuses on the energy management strategies of a micro-grid under construction. In particular, an assessment of system performance is carried out with reference to operational conditions coming from real meteorological data. Three different energy management strategies are compared, two based on the SOC of batteries and a third based on the minimization of operational costs.

2. Modeling of the micro-grid

A laboratory for the study and testing of solar thermal technologies and hydrogen production from renewable sources is under construction at the Renewable Energy Cluster of Sardegna Ricerche, near Cagliari. The main mission of this laboratory is implementation, testing and demonstration of the technologies related to the production, storage and use of hydrogen from RES. The laboratory includes a microgrid powered by RES for hydrogen production, storage and subsequent conversion into electricity by fuel cells. Hydrogen is produced by two PEM electrolyzers and the hydrogen produced is stored in pressurized vessels. Four independent tanks of 1 m^3 each ensure adequate flexibility of the overall system. The stored hydrogen is then used to power a 5 kW PEM fuel cell which produces electrical energy during peaking periods. To study and compare different storage systems, a bank of 32 lead-acid batteries will also be installed. Table 1 shows the main characteristics of the micro-grid devices.

To simulate the behavior of the main components of the micro-grid under different weather conditions and user demand profiles, a specific simulation model was developed. The simulation models of each micro-grid device were implemented in Matlab-Simulink and are described below.

2.1. Photovoltaic system

The modeling of the electrical behavior of the single photovoltaic cell, and thus of the entire system, is performed using the equivalent circuit shown in Fig. 1(a) [8]. The current generator (I_{SC}) simulates the photovoltaic effect which is directly proportional to the solar radiation, the diode in parallel represents the physical behavior of a PN junction, the series resistor (R_S) represents the material resistance, the parallel resistor (R_P) represents the percentage of current that does not reach the external circuit. The equation of cell current (I_{PV}) as a function of voltage (V_{PV}) is:

$$I_{PV} = N_{CELL}\left[I_{SC} - I_0\left(e^{\frac{V_{PV}-R_S I_{PV}}{V_T}} - 1\right) - \frac{V_{PV} - R_S I_{PV}}{R_P}\right] \quad (1)$$

The evaluation of the influence of cell temperature is carried out through the implementation of the thermal balance of the PV module [9]. Fig. 1(b) shows the current/voltage characteristics in function of solar irradiance. The photovoltaic system is appropriately configured in strings of modules in parallel so as to satisfy the demand of the inverter. PV voltage is adjusted by appropriate switching of the DC/DC converter to maximize the average power output of the array. At a given irradiation condition and temperature, the working voltage of the PV system is varied In this paper, the MPPT control is carried out by a function implemented in Matlab. In addition to taking into account the energy losses of the inverter, an efficiency curve provided by the manufacturer is also introduced.

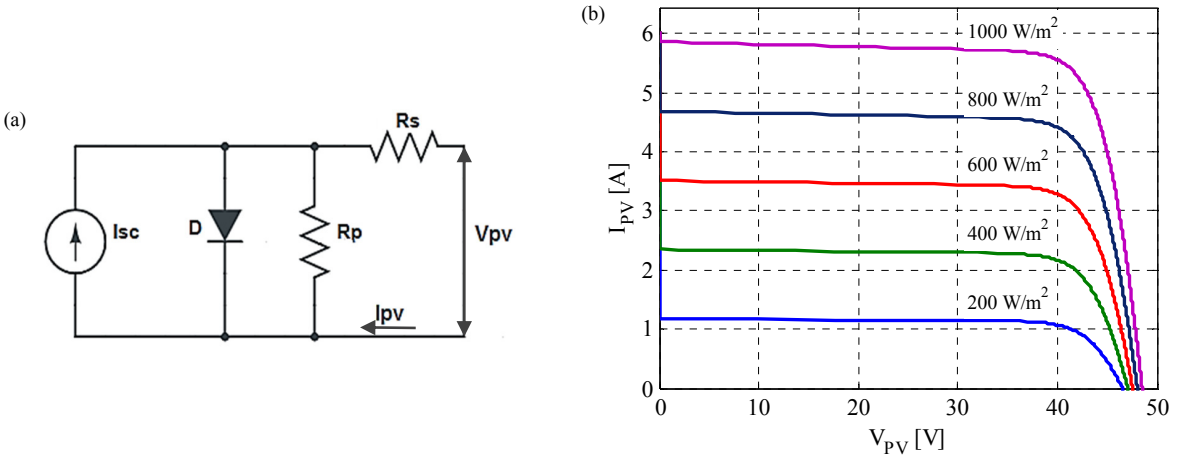

Fig. 1. (a) Equivalent circuit of photovoltaic cell; (b) characteristic curve of photovoltaic panel

2.2. Wind turbine

The power produced by the wind turbine is obtained by the power curve provided by the manufacturer. Fig. 2 shows the wind turbine power curve as a function of wind speed at hub height. A wind shear is modeled to take into account the difference in height between the hub and the anemometer. The wind shear is a function of both altitude and roughness of the ground. The relation used to calculate v_{WT} as a function v_{AN} is:

$$v_{WT} = v_{AN} \cdot \ln\left(\frac{z_{WT}}{z_0}\right) \Big/ \ln\left(\frac{z_{AN}}{z_0}\right) \tag{2}$$

where z_0 is the surface roughness assumed equal to 0.0025 m. Starting from wind speed at hub height, the driving torque generated by the blades on the hub can be calculated through an appropriate control system as the resistant torque of the permanent magnet generator. The electric system is modeled by a voltage generator (indicating the electromotive force generated by the variation of the magnetic field on the coils and directly proportional to the speed of rotation of the machine), a characteristic resistance (to take into account the resistance of the material) and a characteristic inductance (for the presence of coils).

2.3. Batteries

The modeling of the battery is based on an equivalent circuit composed of the series of a voltage source E_B and the internal resistance R_B. The controlled voltage source is a function of output current and the actual battery charge [10]:

$$E_B = E_{B,0} - K\frac{Q_B}{Q_B - I_{B,t}} + A \cdot e^{(-B \cdot I_{B,t})} \tag{3}$$

The values of the equation coefficients are estimated from data provided by the manufacturer and with reference to [10]. An important parameter of the batteries is the state of charge (SOC). It is defined as the ratio between the stored energy and its nominal storage capacity. Fig. 3 shows the curve generated by the model for a discharge current of 12 A, as well as the battery voltage as a function of the SOC of the battery. The inverter/rectifier has the task of controlling and managing the battery bank. As for the PV inverter, the manufacturer provided the inverter efficiency curve as a function of power. A further loss of 10% in addition to inverter losses is assumed in the operation as the rectifier.

2.4. Hydrogen storage system

Through an electrochemical process, the electrolyzer splits water into oxygen and high purity hydrogen. By Faraday's law, the produced hydrogen flow (n_{H2}) is a function of the current (I_{EL}):

$$n_{H2} = \eta_F \frac{N_C I_{EL}}{2F} \quad (4)$$

With reference to literature data [11-13] it was possible to built the characteristic curve of the electrolyzer in function of the current and the operating temperature (Fig. 4). The equation that links the reference voltage and current is:

$$V_{EL} = E_{Nernst}(T_{EL}) + E_{act}(I_{EL}, T_{EL}) + E_{ohm}(I_{EL}, T_{EL}) \quad (5)$$

The main relation used to characterize the electrical behavior of the electrolyzer or fuel cell is the Nernst equation:

$$E_{Nernst} = E_0 + \frac{RT_{FC}}{2F} \cdot \ln\left(\frac{p_{H2}\, p_{O2}^{0.5}}{p_{H2O}}\right) \quad (6)$$

where E_0 is the reversible electric potential in standard conditions (equal to 1.229 V), p_{H2}, p_{O2} and p_{H2O} the hydrogen, oxygen and water vapor partial pressure respectively. The real voltage (V_{EL}) differs from the ideal (E_{Nernst}) mainly due to two irreversible phenomena: the first, felt especially at low current values, is related to activation loss where an overvoltage E_{act} is required to ensure the detaching of formed ions from the electrode. The second phenomenon, related to the ohmic overvoltage term E_{ohm}, arises from cell voltage drop due membrane resistances.

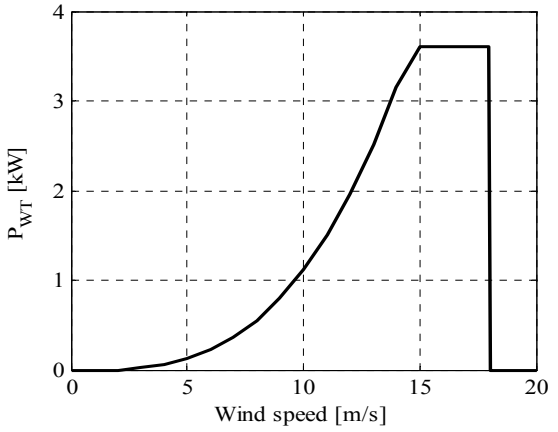

Fig. 2. Wind turbine power curve.

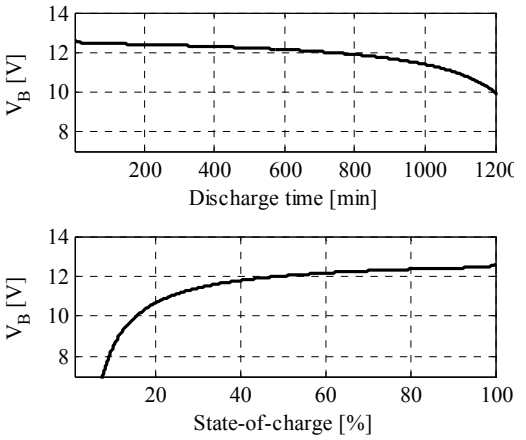

Fig. 3 Battery characteristics.

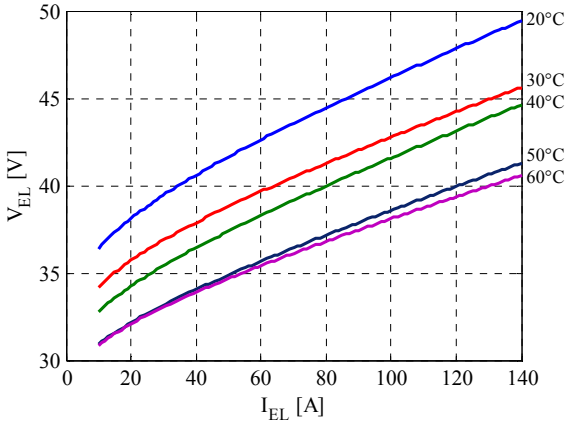

Fig. 4. Electrolyzer characteristic curves

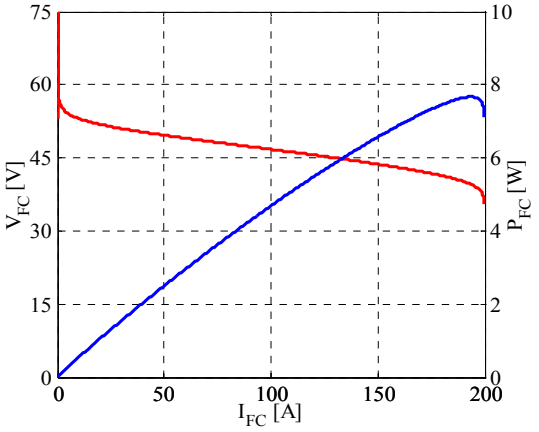

Fig. 5. Fuel cell characteristic curves.

The assessment of the electrolyzer operating temperature is carried out through implementation of the thermal balance of the stack [12]. The hydrogen produced is stored in a storage system consisting of four steel tanks. For the modeling of these devices, the equation of ideal gases with a proper compressibility factor z is used:

$$p_S - p_{atm} = z \cdot \frac{n_{H2} R T_S}{MM_{H2} v_S} \quad (7)$$

where T_S is assumed equal to 40°C and z is a function of tank pressure approximated with a 4th-order polynomial [14].

In the fuel cell the chemical energy of the fuel (hydrogen in this case) is converted to electrical energy through an electrochemical process. The modeling is based on the reconstruction of the characteristic curve and thus the definition of the generator operating point. The real electric potential V_{FC} is given by:

$$V_{FC} = E_{Nernst}(T_{FC}) - E_{act}(I_{FC}, T_{FC}) - E_{ohm}(I_{FC}, T_{FC}) - E_{conc}(I_{FC}) \quad (8)$$

Unlike Eq. (5), in Eq. (8) the irreversible phenomena lead to a voltage drop (with a change in sign) and there is an additional term, E_{conc}, called concentration overvoltage. This overvoltage is felt for high values of current and is due to reagent inability to diffuse into the electrolyte and/or product inability to leave space for new reagents. The estimation of activation, ohmic and concentration overvoltage is carried out by reference [15,16]. Fig. 5 shows the characteristic curve of the fuel cell for an operating temperature of 50°C. The operating temperature of the fuel cell is estimated by the implementation of a heat balance of the generator with reference of [11].

3. Energy management strategies

In this paper three different management strategies are compared. The main objective of this study is to generate an energy management system that can satisfy the following criteria:

- guarantee the electrical energy required by the user load.
- manage efficiently all the equipment;
- minimize the excess energy (energy not used and not stored).

3.1. Energy Management A (EM-A)

The first logic (EM-A) uses the state of battery charge (SOC) as a control variable. Batteries are used for short storage periods while the hydrogen system is used for longer storage periods. In this way, the hydrogen system is secondary to the main role of the batteries and the operating hours of the hydrogen system are significantly reduced. When generated power exceeds the power required by user and SOC is below a predetermined value (called SOC_{EL}), batteries are charged. When the SOC reaches the SOC_{EL} value and the excess power is above the operated electrolyzer minimum power, the electrolyzer is activated until it reaches the maximum pressure inside the hydrogen tanks (p_{H2MAX}). Vice versa, when generated power is less than power required by user, the batteries start to discharge until a minimum value of SOC (SOC_{MIN}) is reached. If the batteries are completely discharged and the amount of hydrogen in the tanks is sufficient, the fuel cell is turned on.

3.2. Energy Management B (EM-B)

Unlike the previous model, in this case both electrolyzer and fuel cell work in nominal conditions when their use is required: the battery bank will compensate for any demands or excesses of power production. In this way, the electrolyzer and the fuel cell can work at maximum efficiency, but energy losses may increase due to the greater use of devices to accumulate and return a certain amount of energy. During the charging phase, if the SOC is above a predetermined level ($SOC_{EL,IN}$), the hydrogen tanks are not fully charged and the excess power is above a certain value (defined as a fraction of the electrolyzer nominal power f) the electrolyzer is switched on and operates under nominal conditions. The batteries compensate for the difference between the excess power and the electrolyzer demands. During the discharge phase, the fuel cell will be turned on when batteries are completely discharged ($SOC<SOC_{MIN}$) and power not used by the load will be used to recharge them. To avoid continuous starting and stopping of the

generator a small hysteresis loop is introduced and the fuel cell will be turned off when the SOC of batteries is higher than predefined level ($SOC>SOC_{FC}$).

3.3. *Energy Management C (EM-C)*

The EM-C energy management strategy is based on the minimization of cost of energy. During the charging phase, the use of batteries or electrolyzer to store the excess power depends on which of the two devices has the lowest cost of cycling energy [6] (i.e. the operating and maintenance cost for 1 h, including depreciation and replacement costs). The cost of cycling the energy through the batteries ($C_{B,CH}$) corresponding to a certain power P, can be calculated as:

$$C_{B,CH} = \frac{C_{B,IN}}{Q_B V_B N_{CYCLES} \eta_B} \cdot P \tag{9}$$

where $N_{B,C}$ is the average battery lifetime in terms of equivalent full cycles, and η_B is the overall efficiency of the batteries including inverter/rectifier efficiency. The cost of cycling the energy through hydrogen storage system is:

$$C_{EL} = \frac{C_{EL,IN}/L_{EL} + C_{O\&M,EL} + C_{FC,IN}/L_{FC} + C_{O\&M,FC}}{\eta_{EL} \cdot \eta_{FC}} \tag{10}$$

During the discharge phase, the selection of the device supplying the energy depends on the associated costs, described as follows. The average cost of supplying a certain power with the batteries for 1 h can be calculated as:

$$C_{B,DIS} = \frac{C_{B,IN}}{Q_B V_B N_{CYCLES} \sqrt{\eta_B}} \cdot P \tag{11}$$

where the battery discharge efficiency is set equal to battery charge efficiency and equal to the square root of the overall efficiency of the batteries η_B. The average cost of supplying power with a fuel cell is:

$$C_{FC} = \frac{C_{FC,IN}/L_{FC} + C_{O\&M,FC}}{\eta_{FC}} \tag{12}$$

4. Case studies and results

The aim of this paper is not to design the components for an isolated renewable energy system, but to study the operation of a given system. For this reason, real meteorological data recorded by a weather station near the system are preferred to statistical data. The data provided are related to solar radiation, wind speed and wind direction at two meters from the ground, atmospheric pressure and ambient temperature and have a sampling time of 30 seconds. As starting case studies, two different climatic situations are identified: a serene summer day (16/07/12) and a cloudy autumn day (02/10/12). With reference to the load profile, real data are not currently available, so a variable load with a 8 h peak period centered at noon is assumed. Values of the required power are obtained by reference to a previous work [17]: a peak load equal to 4200 W and a base load of 800 W for the remaining hours is set (daily energy demand of 46.4 kWh). Table 2 shows the values imposed in the three diagrams, including the initial values of battery charge (SOC_{IN}) and hydrogen pressure inside the tanks ($p_{H2,\,IN}$).

From solar radiation and wind speed conditions, the power produced by the photovoltaic system and wind turbine is known. This power will be used in part directly by the load and in part sent to the two storage systems. Fig. 6 shows the evolution in time of produced power on the summer day ($P_{RES,SUM}$) and the autumn day ($P_{RES,SUM}$) and required power (P_{LOAD}). At the end of the summer day, the total energy produced is equal to 58.8 kWh, (86% produced by photovoltaic and 14% by wind turbine), whereas total energy produced decreases to 23.78 kWh on the autumn day (97% produced by photovoltaic). Daily energy production exceeds the demand (by about 21%) only during the summer day. This energy is partly stored and available for the next day and partly lost due to the inefficiencies of the two storage systems. Instead, on the autumn day the energy produced is almost 50% of the demand: a large amount of stored energy is used to cover this deficit. The results obtained for the 3 energy management strategies previously described are discussed for each case study in the following.

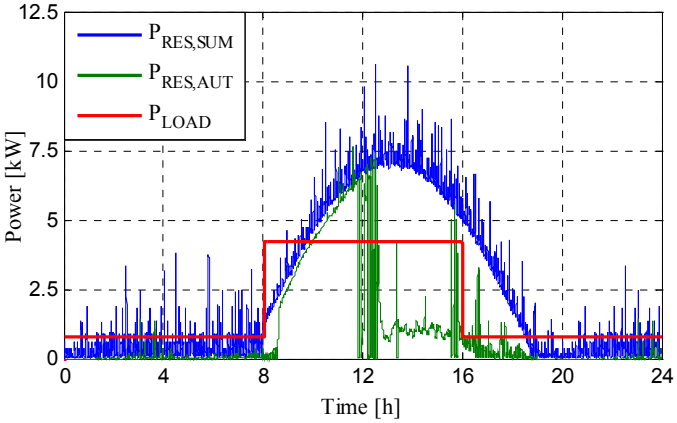

Fig. 6. Daily generated power and load request

Table 2. Limit values imposed.

Battery Bank			
SOC_{IN}	85%	$SOC_{EL,\ IN}$	90%
SOC_{MIN}	70%	SOC_{EL}	98%
SOC_{FC}	80%	SOC_{MAX}	100%
Hydrogen storage system			
$p_{H2,IN}$	7.5 barg	$P_{FC,MIN}$	100 W
$p_{H2,MIN}$	3 barg	$P_{EL,MAX}$	6000 W
$p_{H2,MAX}$	13.8 barg	f	75%

4.1. Summer day case:

Fig. 7(a) shows the simulation results for energy management EM-A. In this case, the hydrogen system is not used and batteries cover any deficit or excess of power. At the end of the day, the SOC of batteries is increased compared with its initial value, reaching almost 90% of charge. Results for energy management EM-B are shown in Fig. 7(b): unlike the previous one, the electrolyzer is used and operates at nominal conditions. At 4 pm $SOC_{EL,\ IN}$ is reached by the batteries and the electrolyzer is turned on to produce hydrogen for about 2 hours. Since the produced power is not sufficient to meet the load and simultaneously to operate the electrolyzer in nominal conditions, part of the energy is supplied by the battery bank. The electrolyzer is turned off when the SOC decreases down to $SOC_{EL,\ IN}$. Finally, Fig. 7(c) shows the result of simulation for energy management EM-C. The trend is similar to Fig. 7(a) but differs at the beginning of the morning when use of the fuel cell is preferred even though the batteries are not fully discharged. This is due to the higher sensitivity of the operational cost of the batteries (Eq. (11)) for the power variation compared to the operational cost of the fuel cell (Eq. (12)).

4.2. Autumn day case:

In this case study, the use of the hydrogen system, especially the fuel cell, is major due to a higher need for power from storage to satisfy the power demand. Fig. 7(d) shows the simulation result for the EM-A logic system. Batteries are used to compensate for the difference between supply and demand until 2 pm when the minimum value of SOC is reached. The fuel cell is switched on and works until the end of the day. Instead, for the EM-B system (Fig. 7(e)), the use of the fuel cell in nominal conditions is required starting from 2 pm and the surplus of energy produced is used to partially recharge the batteries. In this way, the amount of operating hours of the fuel cell decreases and batteries are not completely discharged at the end of the day. Finally, Fig. 7(f) shows the result for the EM-C system: the fuel cell is used to supply most of the required power when the operational cost of the fuel cell is lower than that of the batteries. Around noon there is also a repeated on/off status of the fuel cell mainly due to the fluctuation of the power given by the wind turbine. However, this power fluctuation may lead to failure and reduces the fuel cell lifetime.

5. Conclusion

In this work, attention was focused on the study of the energy management strategies for an isolated micro-grid with hydrogen production and storage under construction. From real meteorological data, the behavior of the system was studied for three different logics in two different weather conditions. Simulation results are summarized in Table 3. The EM-A logic shows the lowest use of the hydrogen system on the summer day and the use of the fuel cell when the batteries are completely discharged on the autumn day.

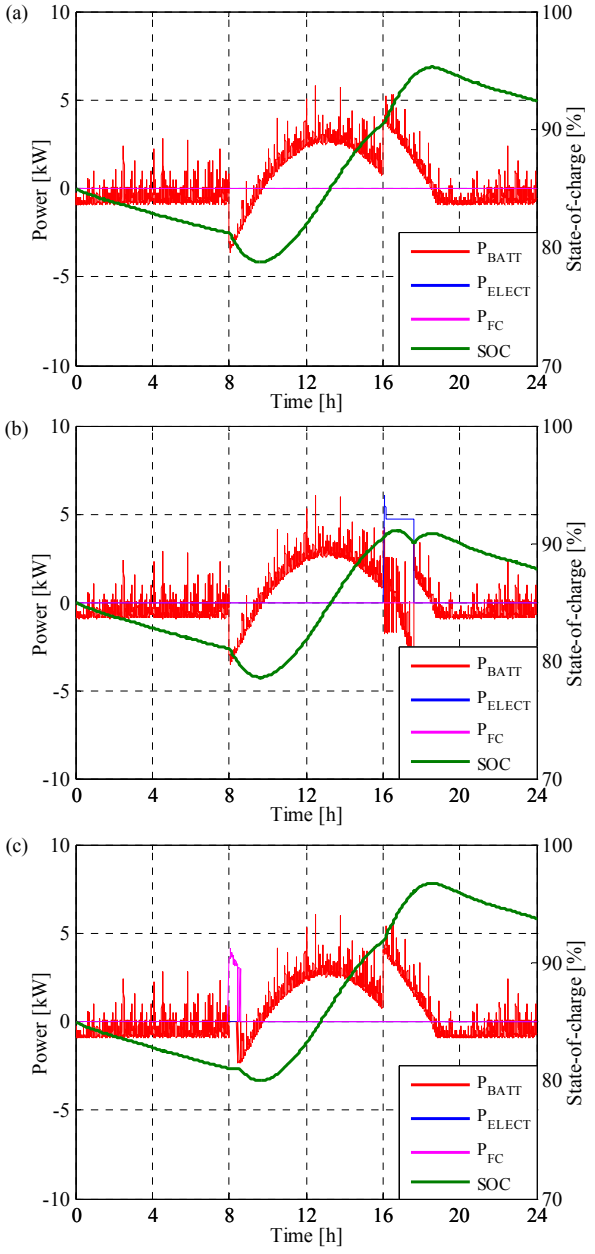

Fig. 7. Simulation results for summer day case and (a) EM-A strategy, (b) EM-B strategy, (c) EM-C strategy.

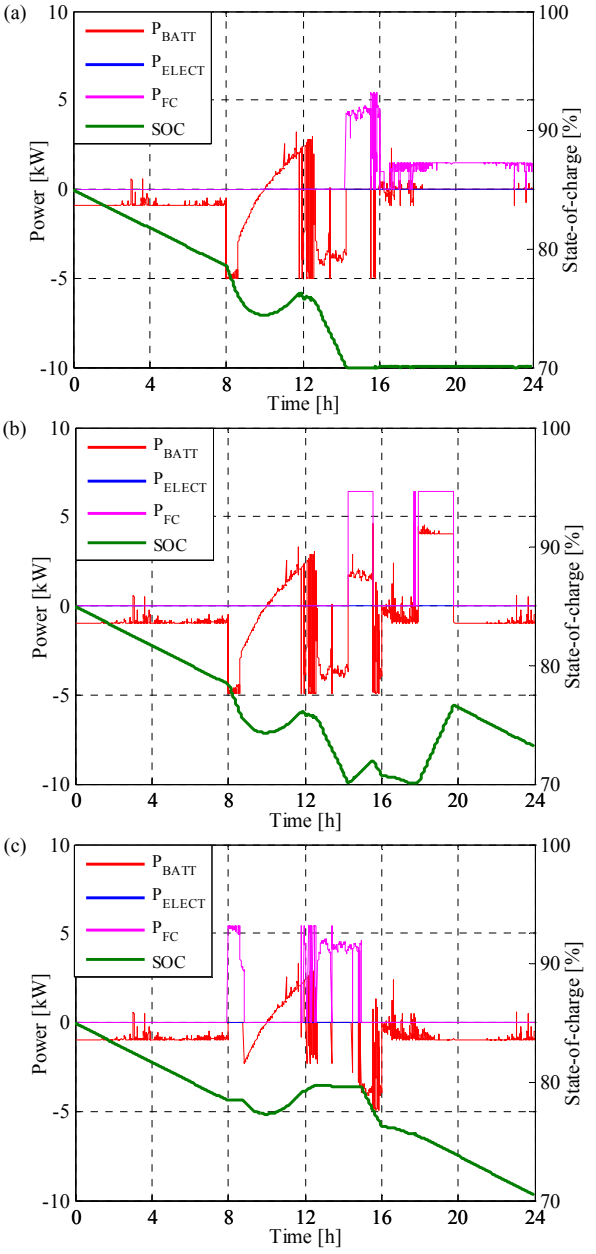

Fig. 8. Simulation results for autumn day casa (and (a) EM-A strategy, (b) EM-B strategy, (c) EM-C strategy.

This fact may give an excessive rigidity to the management system and make the fuel cell work not in the best conditions. With the constraint of operating only in the nominal condition for electrolyzer and fuel cell, the EM-B strategy shows the highest use of the hydrogen storage system. In this case, a suitable hydrogen storage volume will be required to prevent complete filling and emptying of the tanks (such as in the autumn day case) resulting in unavailability of this storage system. Furthermore, this system shows the highest value of energy exchanged with the system at the end of the day (in absolute terms): in the autumn days it can cause major use of storage systems with

increasing energy loss. Finally, the EM-C strategy shows an interesting use of the hydrogen storage system, in particular for the fuel cell, during periods of high power demand. With reference to the autumn scenario, the EM-C strategy leads to the best management with an amount of energy used to cover the deficit between supply and demand at the end of the day lower than in the other two cases. On the other hand, an energy management based on cost minimization is difficult to implement and can cause a continuous on/off status of the devices which may reduce their lifetime.
More comparative elements between the different strategies can be derived by increasing the time horizon of more than a day or extending the analysis to other case studies (coming to an annual analysis).

Table 3. Summary of the results found

Summer day case	**SOC_{FIN}** [%]	**$p_{H2,FIN}$** [bar]	**E_{BATT}** [kWh]	**E_{ELEC}** [kWh]	**E_{FC}** [kWh]	**Autumn day case**	**SOC_{FIN}** [%]	**$p_{H2,FIN}$** [bar]	**E_{BATT}** [kWh]	**E_{ELEC}** [kWh]	**E_{FC}** [kWh]
EM-A	92.5	7.50	9.36	0	0	***EM-A***	70.0	4.34	-18.02	0	-18.61
EM-B	88.0	8.00	3.76	7.52	0	***EM-B***	73.2	3.00	-13.96	0	-22.19
EM-C	93.8	7.13	11.02	0	-2.01	***EM-C***	70.5	4.43	-17.57	0	-16.15

Acknowledgements

This work was carried out as part of a collaboration agreement with the Consortium “Sardegna Ricerche” for the management, scientific coordination and development of research activities of the Laboratory "Concentrated Solar Technologies and Hydrogen from RES".

References

[1] Directive 2009/28/EC of the European Parliament and of the Council, On the promotion of the use of energy from renewable sources and amending and subsequently repealing Directives 2001/77/EC and 2003/30/EC, Official Journal of the European Union, 23 April 2009
[2] Legambiente, Comuni Rinnovabili 2013, Ufficio Energia e Clima di Legambiente, E. Zanchini, K. Eroe, G. Nanni, M. A. Vitelli, Italia, 2013.
[3] Ø. Ulleberg, The importance of control strategies in PV–hydrogen systems, Solar Energy 76, pp. 323-329, 2004.
[4] D. Ipsakis, S. Voutetakis, P. Seferlis, F. Stergiopoulos, C. Elmasides, Power management strategies for a stand-alone power system using renewable energy sources and hydrogen storage, Int. J. Hydrogen Energy 34, pp. 7081-7095, 2009.
[5] E. Dursun, O. Kilic, Comparative evaluation of different power management strategies of a stand-alone PV/Wind/PEMFC hybrid power system, Int. J. Electrical Power & Energy Systems 34, pp. 81-89, 2012.
[6] R. Dufo-López, J.L. Bernal-Agustín, J. Contreras, Optimization of control strategies for stand-alone renewable energy systems with hydrogen storage, Renewable Energy 32, pp. 1102-1126, 2007.
[7] M. Castañeda, A. Cano, F. Jurado, H. Sánchez, L.M. Fernández, Sizing optimization, dynamic modeling and energy management strategies of a stand-alone PV/hydrogen/battery-based hybrid system, Int. J. Hydrogen Energy 38, pp. 3830-3845, 2013.
[8] M.A.S. Masoum, H. Dehbonei, E.F. Fuchs, Theoretical and Experimental Analyses of Photovoltaic Systems with Voltage- and Current-Based Maximum Power-Point Tracking, , IEEE Transaction on Energy Conversion 17, pp. 514-522, 2002.
[9] Y. Sukamongkol, S. Chungpaibulpatana, W. Ongsakul, A simulation model for predicting the performance of a solar photovoltaic system with alternating current loads, Renewable Energy 27, pp. 237-258, 2002.
[10] O. Tremblay, L.A. Dessaint, A.I. Dekkiche, A generic battery model for the dynamic simulation of hybrid electric vehicles, Proc. Vehicle Power and Propulsion IEEE Conference, pp. 284-289, 2007.
[11] Ø. Ulleberg, Stand-alone power system for the future:optimal design, operational and control of solar-hydrogen energy systems, Ph.D. thesis, Norwegian University of Science and Technology, Norway, 1998.
[12] K. Harrison, Design, Integration and Control of Proton Exchange Membrane Electrolyzer for Wind Based Renewable Energy Application, Ph.D. thesis, University of North Dakota, USA, August 2006.
[13] N.V. Dale, M.D. Mann, H. Salehfar, Semiempirical model based on thermodynamic principles for determining 6 kW proton exchange membrane electrolyzer stack characteristics, J. Power Sources 185, pp. 1348-1353, 2008.
[14] L. Zhou, Y. Zhou, Determination of compressibility factor and fugacity coefficient of hydrogen in studies of adsorptive storage, Int. J. Hydrogen Energy 26, pp. 597-601, 2001
[15] M.J. Khan, M.T. Iqbal, Modeling and Analysis of Electrochemical, Thermal, and Reactant Flow Dynamics for a PEM Fuel Cell System, Fuel Cells 4, pp. 463-475, 2005.
[16] A.J. del Real, A. Arce, C. Bordons, Development and experimental validation of a PEM fuel cell dynamic model, J. of Power Sources 173, pp. 310-324, 2007.
[17] G. Cau, D. Cocco, M. Petrollese, V. Tola, Assessment of a hybrid stand-alone power system with hydrogen production and storage, Proc. 3rd International Conference on Microgeneration and Related Technologies, Naples, 2013.